

# Topology-Preserving Adversarial Training

Xiaoyue Mi, Fan Tang, Yepeng Weng, Danding Wang, Juan Cao, Sheng Tang, Peng Li, Yang Liu

**Abstract**—Despite the effectiveness in improving the robustness of neural networks, adversarial training has suffered from the natural accuracy degradation problem, i.e., accuracy on natural samples has reduced significantly. In this study, we reveal that natural accuracy degradation is highly related to the disruption of the natural sample topology in the representation space by quantitative and qualitative experiments. Based on this observation, we propose Topology-pReserving Adversarial traINing (TRAIN) to alleviate the problem by preserving the topology structure of natural samples from a standard model trained only on natural samples during adversarial training. As an additional regularization, our method can easily be combined with various popular adversarial training algorithms in a plug-and-play manner, taking advantage of both sides. Extensive experiments on CIFAR-10, CIFAR-100, and Tiny ImageNet show that our proposed method achieves consistent and significant improvements over various strong baselines in most cases. Specifically, without additional data, our proposed method achieves up to 8.78% improvement in natural accuracy and 4.50% improvement in robust accuracy.

**Index Terms**—Adversarial examples, adversarial training, deep neural network (DNN), robustness.

## I. INTRODUCTION

DEEP neural networks (DNNs) have highlighted the vulnerability to adversarial examples [1]–[5], which are normal data with human imperceptible perturbations [6]. In response, a range of adversarial defense methods has been proposed to enhance the adversarial robustness of DNNs [7]–[12]. Adversarial training [13]–[16] has been proven to effectively improve the robustness of neural networks [17], [18]. However, models trained by adversarial training strategy have shown a significant reduction of accuracy in natural samples [7], which is usually called *natural accuracy degradation* [19]. This problem hinders the practical application of adversarial training, as natural samples are the vast majority in reality [20].

Existing works propose to alleviate natural accuracy degradation by data augmentation or extra data collection [21], distilling classifier boundary of the standard model [19], [22], [23], instance reweighting [24], early-stopping [25], adjustments of loss functions [16], and learnable attack strategies during training [26]. However, the models using adversarial training still have a gap in natural accuracy compared to standard models, which is still an obstacle that limits adversarial training to practical applications.

Xiaoyue Mi, Fan Tang, Yepeng Weng, Danding Wang, Juan Cao, and Sheng Tang are with the Institute of Computing Technology, Chinese Academy of Sciences, Beijing 100190, China, e-mail: {mixi-aoyue19s,tangfan,wengyepeng19s,wangdanding,caojuan,ts}@ict.ac.cn.

Peng Li is with the Institute for AI Industry Research (AIR), Tsinghua University, Beijing 100084, China, e-mail: lipeng@air.tsinghua.edu.cn.

Yang Liu is with the Department of Computer Science and Technology, Tsinghua University, Beijing 100084, China, e-mail: liuyang2011@tsinghua.edu.cn.

Different from previous efforts, we attempt to explain the natural accuracy degradation from a new perspective, topology. Topology refers to the neighborhood relation of data in the representation space, and topology preservation means data that are neighbors in one space should still be neighbors after being projected [27]. And for a classification task, a well-generalizing topology means that both the sample and its near neighbors in the representation space belong to the same class. Various studies [28]–[30] have shown the importance of topology in representation learning, but its impact on adversarial training has not been fully explored.

We conjecture that adversarial training destroys the topology of natural samples in the representation space, which leads to natural accuracy degradation. As illustrated in Fig. 1a, standard training has a well-generalizing topology of natural samples but is vulnerable to adversarial samples. Adversarial samples are usually far from their true class distribution in the representation space, and as shown in Fig. 1b, adversarial training pulls the representation of the adversarial samples and their corresponding natural samples nearer [31]. However, adversarial training enhances the model’s robustness while leading to the poor topological structure of the natural sample features due to the influence of the adversarial samples. Our qualitative and quantitative analyses support the intuition that natural accuracy is strongly correlated with the extent to the topology preservation of natural samples (see Sec. III-B for more details).

Inspired by the above intuition, we propose a new approach called Topology-pReserving Adversarial traINing (TRAIN) to improve adversarial robustness. As shown in Fig. 1c, our goal is to improve the similarities between adversarial and corresponding natural samples in the representation space while preserving the well-generalizing topology of the natural samples. A straightforward solution is to distill the natural sample features of the standard model or the relationships based on the absolute distance between samples during adversarial training. However, it suffers from optimization difficulties due to the great gap between standard and adversarial models. As a result, we construct the topological structure of data in the representation space based on the neighbor graph for each model. We define the edge weight of the graph as the probability that different samples are neighbors, and topology preservation is achieved by aligning the standard model’s graph and the adversarial model’s graph. Experiments show that benefit from topology preservation, TRAIN improves both the classification accuracy on natural samples and the robustness performance through combination with other adversarial training algorithms in a plug-and-play way.

Our contributions are as follows:

- We reveal that the topology of natural samples in the representation space plays an important role in the natural

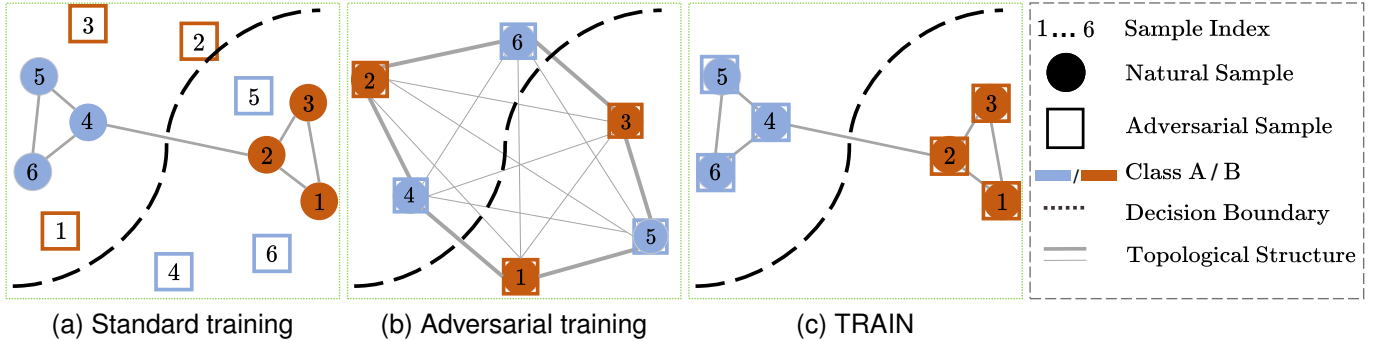


Fig. 1. Illustrations for representation space under different training conditions. The sample index of the adversarial sample and its corresponding natural sample are the same. The color indicates the true category of the sample. A thicker line indicates a higher probability that two points are neighbors. (a) In the representation space of the standard training, the natural samples are clearly separated and have a well-generalizing topology (natural), but the corresponding adversarial samples are far and misclassified. (b) The adversarial training representation is more robust to adversarial attacks. Still, the natural data representations are negatively affected by the adversarial ones, and the topological structure is destroyed. (c) Our method TRAIN preserves the well-generalizing topology while bringing natural and adversarial representations together, thus forming a robust and discriminative representation space.

accuracy of adversarial models, which provides a new perspective on mitigating natural accuracy degradation.

- We propose a *topology preservation adversarial training* method that preserves the topological structure between natural samples from the standard model’s representation space, which can be combined with various adversarial training methods in a plug-and-play manner.
- Extensive quantitative and qualitative experiments on CIFAR-10, CIFAR-100, and Tiny ImageNet datasets show the effectiveness of the proposed TRAIN (maximum 8.78% improvement for the natural accuracy and 4.50% for the robust accuracy).

## II. RELATED WORK

### A. Adversarial Training

Adversarial training is known as one of the most effective methods to improve the adversarial robustness of DNNs. Most adversarial training algorithms [7], [10], [26], [32]–[35] focused on getting natural samples close to the representation of the adversarial samples they generate. Vanilla AT [7] generated adversarial examples by the PGD attack method as model input during training. And based on that, Zhang *et al.* [10] proposed TRADES by punishing the model for outputting different logits of adversarial examples and their corresponding natural images, which as a regularization term adding to the cross-entropy loss. Considering the influence of misclassified data, Wang *et al.* [32] introduced Misclassification Aware adversarial Training (MART), which emphasizes misclassified examples by higher weights. Due to the large computational cost of adversarial training, some approaches [33], [35] use single-step attacks to obtain adversarial examples that greatly reduce training time. Furthermore, Wu *et al.* [34] improved the adversarial robustness by flattening the weight loss landscape. Nevertheless, these methods are subject to the issue of natural accuracy degradation, which is a major obstacle in their practical applications.

Natural accuracy degradation, often referred to as “the trade-off between robustness and accuracy”, is a phenomenon observed in adversarial training that results in a reduction in

the accuracy of natural samples while concurrently increasing adversarial robustness when compared with standard training. Several works have been proposed to alleviate this problem. Zhang *et al.* [25] used early-stopping. Rebuffi *et al.* [21] tried to use more training data by data augmentation or adding extra data. Researchers [19], [22], [23] tried to distill the natural sample logits from the standard model to the adversarial model. Zhang *et al.* [24] made use of instance reweighting. Pang *et al.* [16] redefined adversarial training optimization goals. And Jia *et al.* [26] used reinforcement learning to obtain learnable attack strategies. Different from them, we mitigate this problem from the view of the topology of different data in the representation space.

### B. Knowledge Distillation in Adversarial Training

Knowledge distillation can transfer the ability of the teacher network to the student network and is often used to achieve model compression. Existing knowledge distillation can be divided into three types, logit-based distillation [36], [37], which is limited by label space; feature-based distillation [38]–[40], which is limited by model architecture and feature dimension; and relationship-based distillation [41]–[44] transfers the inter-sample relationships from the teacher model to the student model. The experimental section also includes comparative evaluations of different knowledge distillation methods.

Recently some algorithms have applied knowledge distillation to adversarial training. Some works [45], [46] distilled large robust models for robust model compression. Different from them, researchers [19], [22], [23] distilled the natural data logits of the standard model to enhance adversarial training on natural accuracy. Chen *et al.* [23] considered additional temperature factors during distillation. However, they did not constrain the topology of samples in the representation space, and their distillation loss updates both standard and adversarial models simultaneously. Therefore, they were still negatively affected by adversarial examples.

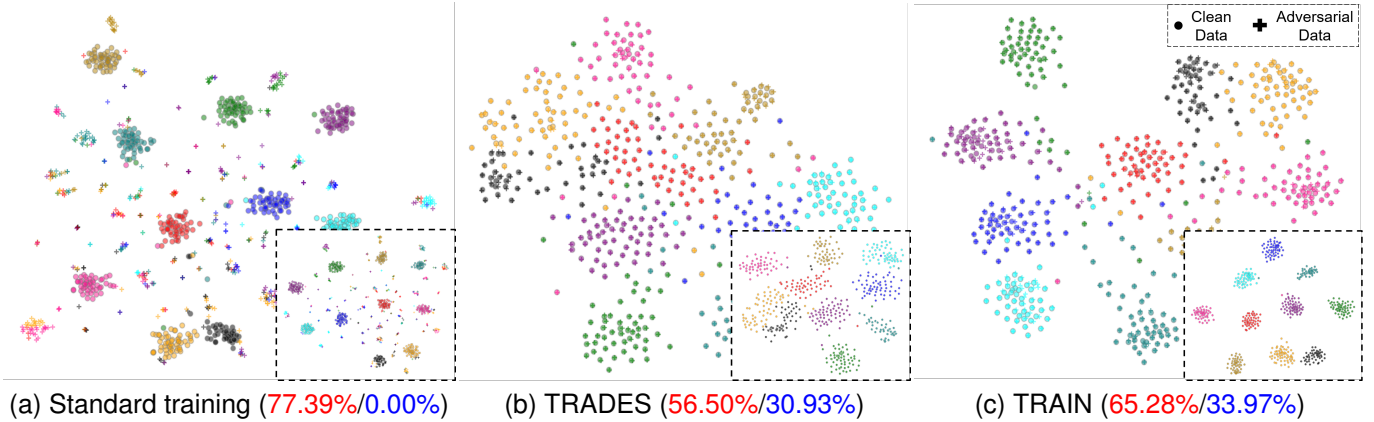


Fig. 2. Analytical experiments on adversarial strength and topology quality in the representation space. We can find that the quality of the topology is closely related to natural accuracy, while adversarial training can destroy the topology of natural samples. (a), (b) and (c) show the difference in the representation space between the standard model, adversarial model (trained by TRADES with  $\beta = 6.0$ ), and TRAIN on CIFAR-100 training set (small plots) and test set (big plots). The red value is the natural accuracy, and the blue value is the PGD-20 accuracy. The penultimate layer of features of the network is visualized using t-SNE.

### C. Topology in Representation Learning

The importance of topology in representation learning has been demonstrated in a number of works [28]–[30], [47], [48]. Belkin *et al.* [28] pointed out that the geometric properties of the representation space strongly influence the model generalization performance. Manifold learning algorithms [29], [47] considered that the priority objective of dimensionality reduction is retaining the topology of the manifold of the high dimensional space. In continual learning, it has been demonstrated that preserving topology can be an effective strategy for mitigating catastrophic forgetting [30], [48]. However, the methods used to construct the topology in these efforts are either computationally intensive or require additional network structures, neither of which are suitable for direct use in adversarial training, which is already consuming significant computational resources.

## III. EFFECT OF TOPOLOGY ON NATURAL ACCURACY

### A. Formulation

Following vanilla AT [7], the goal of adversarial training is defined as:

$$\arg \min_{\theta} \mathbb{E}_{(x,y) \in D} \left( \max_{\delta \in S} L(x + \delta, y; \theta) \right), \quad (1)$$

where  $D$  is the data distribution for input  $x$  and its corresponding label  $y$ ,  $\theta$  is the model parameters.  $\delta$  stands for the perturbation applied to  $x$  and is usually limited by perturbation size  $\epsilon$ .  $S = \{\delta \mid \|\delta\|_p \leq \epsilon\}$  is the feasible domain for  $\delta$ .  $L(\cdot)$  usually is the cross-entropy loss for classification. By min-max gaming, adversarial training aims to correctly recognize all adversarial examples ( $x' = x + \delta$ ).

TRADES [10] improves classification performance by introducing a regularization term, which penalizes the discrepancy between the logits for adversarial examples and their corresponding natural images. Its optimization objective is defined as:

$$\arg \min_{\theta} \mathbb{E}_{(x,y) \in D} \left( L(x, y; \theta) + \beta \max_{\delta \in S} L(x + \delta, x; \theta) \right), \quad (2)$$

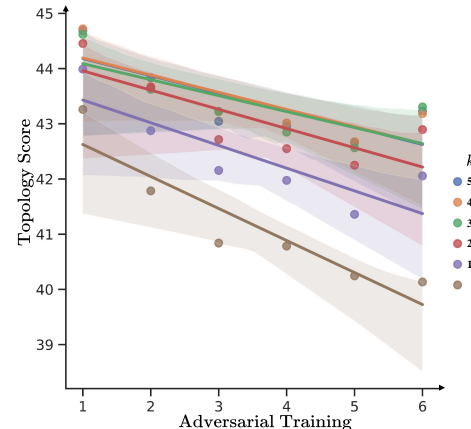


Fig. 3. Quantitative analysis reveals a negative correlation between the adversarial strength, represented by the hyperparameter  $\beta$  in TRADES, and the topology score. Specifically, a higher  $\beta$  value imposes stronger constraints on the alignment of the representations of natural and adversarial samples. Inspired by manifold learning, the topology score is evaluated by  $k$ NN test accuracy. See more details in Sec. III-B.

where  $\beta$  is a hyper-parameter and its value means the strength of regularization for robustness. TRADES has proven highly effective and remains a strong baseline for adversarial training to this day.

For descriptive purposes, we refer to models trained only on natural samples as *standard models* and those trained using adversarial training as *adversarial models* in the latter part.

### B. Empirical Analysis

In this section, we analyze how adversarial training influences topological relationships compared with standard models. We find that the quality of the topology is positively correlated with natural accuracy, while the adversarial strength is negatively correlated with the quality of the topology. Adversarial models are trained by TRADES [10], and here we consider the weights of the adversarial loss function  $\beta$  as adversarial strength. Larger

$\beta$  represents the greater strength of adversarial training. See Sec. V-A for more details of experimental settings.

**Qualitative analysis.** We choose the penultimate layer representations (before logits) of the standard model and adversarial models for qualitative and quantitative experimental analysis. As shown in Fig. 2, compared with the standard model both on the test set and training set, the representation visualization for adversarial models shows more robustness, but worse topology of data resulting in lower discrimination in different classes.

**Quantitative analysis.** To accurately analyze the correlation between adversarial strength and the topological relationship between samples, we conduct quantitative analysis by setting the  $\beta = 1, 2, \dots, 6$  for TRADES. We use  $k$ NN to evaluate the quality of topology for different models, which is often used in manifold learning [29], [47] to evaluate the quality of topological structure during dimension reduction. Specifically, we first use PGD-20 ( $\epsilon = 0.031$ ) [7] to generate adversarial data for the CIFAR-100 dataset, then we use both natural and adversarial data in the training set as the support set to predict the labels of all the examples in the test set. To verify the reliability of the observation conclusion, we choose  $k = 5, 10, 20, 30, 40, 50$ , respectively. Finally, the  $k$ NN accuracy is used as the *topology score* for the learned representation space. The higher the score, the more reasonable the topological relationship between the samples. Fig. 3 shows the strength of adversarial training and their corresponding topology qualities for different  $k$ . A negative correlation between the strength of adversarial training and the topology quality between samples could be observed. Tables I and II show the positive correlation between topology quality and natural accuracy on the CIFAR-10 and CIFAR-100 datasets.

**Why does adversarial training destroy topological relationships?** Adversarial representations are usually far away from their true class distribution. Therefore, the existing adversarial training algorithms will make the representation of natural samples further away from true class distribution while narrowing the adversarial representations and natural representations. Compared with the standard model, the topological relationship between samples of the adversarial model is worse and the representation space of the adversarial model shows lower discrimination in different classes. Zhang *et al.* [24] points out that adversarial training is equivalent to a special kind of regularization and has a strong smoothing effect, which also supports our intuition.

## IV. TOPOLOGY-PRESERVING ADVERSARIAL TRAINING

### A. Overall Framework

To reduce the negative impact of adversarial samples, we propose a method TRAIN that focuses on preserving the topology of natural features from the standard model during adversarial training. As shown in Fig. 4 and Alg. 1, we train two models simultaneously: a standard model  $M$  with a cross-entropy loss  $L_{ST}(\cdot)$  and an adversarial model  $M'$  which is updated by a specific adversarial training algorithm. For natural sample  $x_i$ , the outputs of  $M(x_i)$  are the feature of the last layer  $f_{x_i}$  and logit  $logit_{x_i}$ . Similarly, the outputs of  $M'(x'_i)$

are  $f'_{x'_i}$  and  $logit'_{x'_i}$  for adversarial sample  $x'_i$  and  $f'_{x_i}$  and  $logit'_{x_i}$  for natural sample  $x_i$ .

The loss  $L_{ST}(\cdot)$  of  $M$  is formulated as:

$$L_{ST} = L(z_{x_i}, y_i), z_{x_i} = \frac{e^{logit_{x_i}}}{\sum_{j=1}^N logit_{x_j}}, \quad (3)$$

where  $L$  is cross-entropy loss. And the overall loss  $L_{AT}(\cdot)$  of  $M'$  is formulated as follows:

$$L_{AT} = L_{robust}(x') + \lambda L_{TP}(M, M'), \quad (4)$$

where  $L_{robust}(\cdot)$  denotes the adversarial robustness loss, which is determined by the specific adversarial training algorithm employed. Additionally  $L_{TP}(\cdot)$  serves as a regularization item to preserve the topology of natural samples from  $M$  and updates only  $M'$ . A comprehensive discussion regarding the specifics of  $L_{TP}(\cdot)$  will be discussed in the next subsection.

### B. Topology Preservation in Adversarial Training

The topological structure is typically based on a neighborhood relation graph constructed by the similarity among samples in the representation space [27], [29], [47]. In this graph, each point is a sample in the representation space, while the edges are relationships among the samples, and the weights assigned to the edges are determined by the similarity between the samples. Consequently, the topology preservation can be precisely formulated as follows:

$$L_{TP} = \mathbb{E}_{(x,y) \in D} (F(P, Q)), \quad (5)$$

where  $P$  and  $Q$  represent the neighborhood relation graph constructed by the inter-sample similarity for  $M$  and  $M'$ , respectively.  $F(\cdot)$  measures the similarity between two graphs.

**Absolute relationship preservation.** Directly applying cosine similarity to calculate the pairwise distances  $d_{ij}$  and  $d'_{ij}$  between samples within the high-dimensional representation spaces of  $M$  and  $M'$  to construct the neighborhood relation graph  $P$  and  $Q$  is a straightforward way:

$$P = \{d_{ij} | 0 < i, j \leq N\}, Q = \{d'_{ij} | 0 < i, j \leq N\}, \quad (6)$$

where  $d_{ij}$  and  $d'_{ij}$  are defined as:

$$d_{ij} = 1 - \frac{f_{x_i}^T f_{x_j}}{\|f_{x_i}\|_2 \|f_{x_j}\|_2}, \tilde{d}'_{ij} = 1 - \frac{f'_{x'_i}{}^T f'_{x'_j}}{\|f'_{x'_i}\|_2 \|f'_{x'_j}\|_2}. \quad (7)$$

However, there exists a substantial difference in the representation space between the adversarial model and the standard model, making it challenging to optimize the preservation of direct absolute relationships.

**Relative relationship preservation.** Considering the significant gap between standard and adversarial models, our objective is to use conditional probability distribution for modeling the relationships between samples. Specifically, we define the edge weights of the neighborhood relation graph as the probability that distinct samples are neighbors, thus ensuring topology preservation through the alignment of the probability distributions of the two graphs.

Different from manifold learning [29], [47] which makes use of the regular Kernel Density Estimation (KDE) for

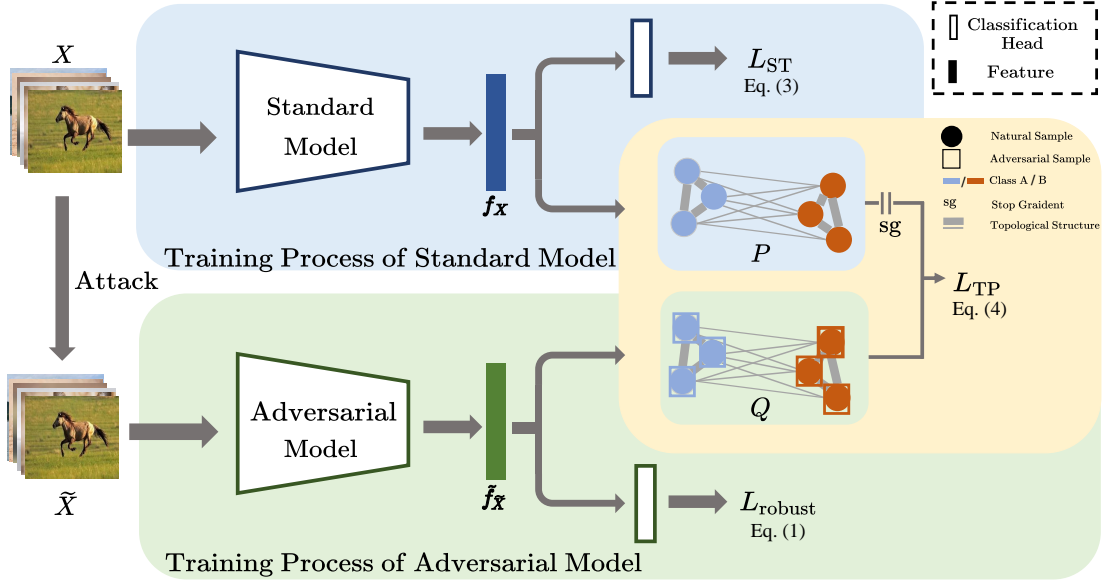


Fig. 4. Overall framework of TRAIN. Specifically, we train a standard model  $M$  and an adversarial model  $M'$ . The standard model takes natural samples  $X$  as input and is optimized by cross-entropy loss. On the other hand, the adversarial model takes adversarial samples  $X'$  as input and is optimized by robust loss  $L_{robust}(\cdot)$  and topology preservation loss  $L_{TP}(\cdot)$ .  $L_{TP}(\cdot)$  constructs and aligns the neighborhood relation graph  $P$  and  $Q$  in the representation spaces of  $M$  and  $M'$ , respectively. It can preserve the topological relationships among samples to reduce the negative effects of the adversarial samples during adversarial training.

approximations of the conditional probabilities, we use the cosine similarity-based affinity metric. This choice is motivated by the excessive hyper-parameter tuning requirements and unacceptable training costs associated with KDE in adversarial training.

$$K_{cos}(f_{x_i}, f_{x_j}) = \frac{1}{2} \left( \frac{f_{x_i}^T f_{x_j}}{\|f_{x_i}\|_2 \|f_{x_j}\|_2} + 1 \right) = \frac{1}{2} (2 - d_{ij}), \quad (8)$$

where  $K_{cos}$  is cosine similarity-based affinity metric value for  $x_i$  and  $x_j$ .

Moreover, we add a special term  $\rho_j$  to better preserve the global structure of representation space.  $\rho_j$  represents the distance from the  $j_{th}$  data point to its nearest neighbor. Subtracting  $\rho_j$  ensures the local connectivity of the graph, avoiding isolated points and thus better preserves the global structure.

$$\tilde{d}_{ij} = d_{ij} - \rho_j, \quad \tilde{d}'_{ij} = d'_{ij} - \rho'_j. \quad (9)$$

After normalization, we obtain the  $p_{i|j}$ , which represents the conditional probability that the  $i_{th}$  natural sample is a neighbor of the  $j_{th}$  natural sample in the representation space of  $M$ .

$$p_{i|j} = \frac{2 - \tilde{d}_{ij}}{\sum_{k=1, k \neq j}^N (2 - \tilde{d}_{jk})}. \quad (10)$$

Similarly, for the adversarial model  $M'$ :

$$q_{i|j} = \frac{2 - \tilde{d}'_{ij}}{\sum_{k=1, k \neq j}^N (2 - \tilde{d}'_{jk})}. \quad (11)$$

So the neighborhood relation graph construction of  $M$  can be formalized as:

$$P = \left\{ p_{i|j} \mid p_{i|j} = \frac{2 - \tilde{d}_{ij}}{\sum_{k=1, k \neq j}^N (2 - \tilde{d}_{jk})}, 0 < i, j \leq N \right\}. \quad (12)$$

Similarly, the relationship graph for  $M'$  is:

$$Q = \left\{ q_{i|j} \mid q_{i|j} = \frac{2 - \tilde{d}'_{ij}}{\sum_{k=1, k \neq j}^N (2 - \tilde{d}'_{jk})}, 0 < i, j \leq N \right\}. \quad (13)$$

We use cross-entropy loss to measure the similarity of  $P$  and  $Q$  for such flexible relationships. Finally, the  $L_{TP}$  for TRAIN is formalized as:

$$L_{TP} = CE(P, Q) = \sum_i \sum_j \left[ p_{i|j} \log \left( \frac{p_{i|j}}{q_{i|j}} \right) + (1 - p_{i|j}) \log \left( \frac{1 - p_{i|j}}{1 - q_{i|j}} \right) \right]. \quad (14)$$

To make it easier for the reader to understand our method, Fig. 4 shows the overall process for TRAIN combined with vanilla AT.

### C. The Flexibility of TRAIN

Different from other methods, TRAIN mitigates natural accuracy degradation by adopting a novel topological perspective. Moreover, TRAIN could be applied to other adversarial training methods, such as vanilla AT [7], TRADES [10], and LBGAT [19], in a plug-and-play way. To validate the effectiveness of our proposed enhancements, we conduct comprehensive validation experiments on these strong baselines. We have introduced the robust loss of vanilla AT and TRADES in Sec. IV-A. Here we will elucidate the specifics of our approach when integrated with another strong baseline LBGAT.

---

**Algorithm 1** Topology-Preserving Adversarial Training
 

---

**Require:** the step size of perturbations  $\epsilon$ , batch size  $n$ , learning rate  $\alpha$ , attack algorithm optimization iteration times  $K$ , the number of training epochs  $T$ , adversarial model  $M'$  with its parameters  $\theta'$ , standard model  $M$  with its parameters  $\theta$ , loss weight  $\lambda$  and training dataset  $(x, y) \in D$

**Ensure:** robust model  $M'$  with  $\theta'$

- 1: Randomly initialize  $\theta, \theta'$
  - 2: **for**  $i = 1, \dots, T$  **do**
  - 3: Sampling a random mini-batch  $X = \{x_1, x_2, \dots, x_n\}$  and corresponding labels  $Y = \{y_1, y_2, \dots, y_n\}$  from  $D$
  - 4: Generating adversarial data  $X' = \{x'_1, x'_2, \dots, x'_n\}$  through attack algorithms (such as PGD-K, FGSM)
  - 5:  $f_X, \text{logit}_X = M(X)$
  - 6:  $f'_{X'}, \text{logit}'_{X'} = M'(X')$
  - 7: Evaluate  $L_{ST}$  Eq. (3)
  - 8: Evaluate  $L_{AT} = \lambda L_{TP} + L_{\text{robust}}$  Eq. (4)
  - 9: Update model parameters:
  - 10:  $\theta = \theta - \alpha \frac{1}{n} \sum_{i=1}^n \nabla_{\theta} L_{ST}$
  - 11:  $\theta' = \theta' - \alpha \frac{1}{n} \sum_{i=1}^n \nabla_{\theta'} L_{AT}$
  - 12: **end for**
- 

LBGAT leverages the model logits obtained from a standard model to guide the learning process of an adversarial model. It is usually combined with vanilla AT and TRADES. The total loss  $L_{AT}$  of adversarial model  $M'$  combined with LBGAT and vanilla AT is:

$$L_{AT} = L(z'_{x'_i}, y_i) + \gamma \| \text{logit}'_{x'_i} - \text{logit}_{x_i} \|_2 + \lambda \sum_i \sum_j \left[ p_{i|j} \log \left( \frac{p_{i|j}}{q_{i|j}} \right) + (1 - p_{i|j}) \log \left( \frac{1 - p_{i|j}}{1 - q_{i|j}} \right) \right], \quad (15)$$

and the total loss of adversarial model  $L_{AT}$  combined with LBGAT and TRADES is:

$$L_{AT} = L(z'_{x'_i}, y_i) + \beta KL(z'_{x'_i} \| z'_{x'_i}) + \gamma \| \text{logit}'_{x'_i} - \text{logit}_{x_i} \|_2 + \lambda \sum_i \sum_j \left[ p_{i|j} \log \left( \frac{p_{i|j}}{q_{i|j}} \right) + (1 - p_{i|j}) \log \left( \frac{1 - p_{i|j}}{1 - q_{i|j}} \right) \right],$$

$$z'_{x_i} = \frac{e^{\text{logit}'_{x_i}}}{\sum_{j=1}^N \text{logit}'_{x_j}}, z'_{x'_i} = \frac{e^{\text{logit}'_{x'_i}}}{\sum_{j=1}^N \text{logit}'_{x'_j}}, \quad (16)$$

where  $KL$  is Kullback–Leibler divergence, which is commonly used to concretely implement the robust regularization of TRADES.  $\gamma$  is the hyper-parameter of LBGAT, and  $\beta$  is the hyper-parameter of TRADES.

**Discussion.** LBGAT also adopts a two-model framework and transfers the prior knowledge of  $M$  to  $M'$ . Nonetheless, there exist notable distinctions between our proposed method and LBGAT, which can be summarized as follows:

- 1) Different perspectives. LBGAT mitigates natural accuracy degradation by focusing on the guidance of the natural classifier boundary. Different from it, our proposed TRAIN emphasizes the importance of the topology of the sample in the representation space. By combining

the two perspectives, we can further enhance the model's performance, as confirmed by the experimental results.

- 2) Different interactions between models. In LBGAT,  $M$  and  $M'$  affect each other which still has the negative impact of the adversarial samples on the natural samples. However, when  $M$  remains independent, optimizing LBGAT becomes challenging due to the inherent differences between the two models. In TRAIN,  $M$  unidirectionally influences  $M'$  and as an anchor to preserve the original topology of natural samples in the representation space to avoid the negative influence of the adversarial samples on the natural samples. This design choice effectively mitigates the adverse effects of adversarial samples on natural samples.

These differentiating factors highlight the unique contributions of our proposed TRAIN method in addressing the natural accuracy degradation during adversarial training. By considering the topological aspects of samples to avoid the negative impact of adversarial samples, TRAIN offers a novel and effective approach for enhancing model robustness and performance.

## V. EXPERIMENTS

### A. Experimental Settings

**Datasets.** In line with state-of-the-art adversarial training methods [16], [19], [26], we conduct extensive evaluations on popular datasets, including CIFAR-10, CIFAR-100 [49] and Tiny ImageNet [50] dataset to validate the effectiveness of our algorithm. The CIFAR-10 and CIFAR-100 datasets consist of a total of 60,000 color images with dimensions of  $32 \times 32$  pixels. Among these 50,000 images are designated for training and the remaining 10,000 images are reserved for testing. Furthermore, CIFAR-10 has 10 categories while CIFAR-100 has 100 categories. Furthermore, the Tiny ImageNet dataset includes 120,000 color images with dimensions of  $64 \times 64$  pixels in 200 categories, with each category containing 500 training images, 50 validation images, and 50 testing images. This dataset offers a larger image size and a broader range of categories, enabling a more challenging evaluation of our algorithm's performance.

**Baselines.** We choose three strong baselines to demonstrate the effectiveness of our method: Vanilla AT [7], TRADES [10], and LBGAT. For TRADES, we set  $\beta = 6.0$ . For LBGAT, we conduct experiments based on vanilla AT and TRADES ( $\beta = 6.0$ ). We also add ALP [51] as a baseline in the Tiny ImageNet dataset. In addition, we combine TRAIN with them to demonstrate the superiority of our approach. To provide a comprehensive evaluation and comparison with other state-of-the-art adversarial training methods, we include additional baseline: MART [32], FAT [25], GAIRAT [24], AWP [34], SAT [52], and LAS [26].

**Evaluation metrics.** To evaluate the generalization of the model on natural and adversarial samples, our evaluation metrics are natural data accuracy (Natural Acc.) and robust accuracy (Robust Acc.). Robust accuracy is the model classification accuracy under adversarial attacks. As specified in the respective publications, we choose three representative

TABLE I

RESULTS ON CIFAR-10. WHEN ADDED TO THE EXISTING BASELINE UNDER MOST SETTINGS, OUR METHOD ACHIEVES BOTH NATURAL ACCURACY AND ROBUST ACCURACY IMPROVEMENTS, PARTICULARLY IN TERMS OF C&W-20 ACC. “\*\*” ARE THE RESULTS DIRECTLY QUOTED FROM LBGAT.

Defense	Natural Acc.	PGD-20 Acc.	Robust Acc. C&W-20 Acc.	AA Acc.	Topology Score	
					Natural	Robust
Standard Training	94.46	0.00	0.00	0.00	94.94	-
Vanilla AT [7]	86.69	53.45	53.72	48.95	86.51	53.94
Vanilla AT + TRAIN	<b>88.85</b> ( $\uparrow$ 2.16)	<b>55.64</b> ( $\uparrow$ 2.19)	<b>56.18</b> ( $\uparrow$ 2.46)	<b>50.89</b> ( $\uparrow$ 1.94)	<b>89.11</b> ( $\uparrow$ 2.60)	<b>56.55</b> ( $\uparrow$ 2.61)
Vanilla AT + LBGAT [19]	86.55	54.34	53.35	47.27	86.64	54.26
Vanilla AT + LBGAT + TRAIN	<b>89.42</b> ( $\uparrow$ 2.87)	<b>56.21</b> ( $\uparrow$ 1.87)	<b>57.48</b> ( $\uparrow$ 4.13)	<b>51.77</b> ( $\uparrow$ 4.50)	<b>89.25</b> ( $\uparrow$ 2.61)	<b>56.59</b> ( $\uparrow$ 2.33)
TRADES* [10]	84.42	56.59	54.91	51.91	85.58	56.73
TRADES + TRAIN	<b>87.30</b> ( $\uparrow$ 2.88)	<b>58.20</b> ( $\uparrow$ 1.61)	<b>56.31</b> ( $\uparrow$ 1.40)	<b>53.09</b> ( $\uparrow$ 1.18)	<b>90.01</b> ( $\uparrow$ 4.43)	<b>58.86</b> ( $\uparrow$ 2.13)
TRADES + LBGAT* [19]	81.98	<b>57.78</b>	55.53	53.14	84.57	57.79
TRADES + LBGAT + TRAIN	<b>87.62</b> ( $\uparrow$ 5.64)	57.73( $\downarrow$ 0.05)	<b>58.08</b> ( $\uparrow$ 2.55)	<b>53.64</b> ( $\uparrow$ 0.50)	<b>89.50</b> ( $\uparrow$ 5.00)	57.98( $\uparrow$ 0.19)

TABLE II

RESULTS ON CIFAR-100. SIMILAR TO TABLE I, OUR METHOD CAN IMPROVE THE NATURAL ACCURACY (UP TO 8.78%), ROBUST ACCURACY (UP TO 3.04%), AND TOPOLOGY SCORE (UP TO 13.21%) OF BASELINES. “\*\*” ARE THE RESULTS DIRECTLY QUOTED FROM LBGAT.

Defense	Natural Acc.	PGD-20 Acc.	Robust Acc. C&W-20 Acc.	AA Acc.	Topology Score	
					Natural	Robust
Standard Training	77.39	0.00	0.00	0.00	77.07	-
Vanilla AT [7]	60.44	28.06	27.85	24.81	57.17	31.32
Vanilla AT + TRAIN	<b>66.39</b> ( $\uparrow$ 5.95)	<b>29.88</b> ( $\uparrow$ 1.82)	<b>29.84</b> ( $\uparrow$ 1.99)	<b>25.81</b> ( $\uparrow$ 1.00)	<b>64.70</b> ( $\uparrow$ 7.53)	<b>32.84</b> ( $\uparrow$ 1.52)
Vanilla AT + LBGAT [19]	61.01	<b>30.10</b>	28.09	25.63	61.28	30.47
Vanilla AT + LBGAT + TRAIN	<b>68.20</b> ( $\uparrow$ 7.19)	29.83( $\downarrow$ 0.27)	<b>30.84</b> ( $\uparrow$ 2.75)	<b>25.88</b> ( $\uparrow$ 0.25)	<b>66.08</b> ( $\uparrow$ 4.80)	<b>32.48</b> ( $\uparrow$ 2.01)
TRADES* [10]	56.50	30.93	28.43	26.87	52.57	32.17
TRADES + TRAIN	<b>65.28</b> ( $\uparrow$ 8.78)	<b>33.97</b> ( $\uparrow$ 3.04)	<b>30.86</b> ( $\uparrow$ 2.43)	<b>28.25</b> ( $\uparrow$ 1.38)	<b>65.78</b> ( $\uparrow$ 13.21)	<b>34.53</b> ( $\uparrow$ 2.36)
TRADES + LBGAT* [19]	60.43	35.50	31.50	<b>29.34</b>	61.06	37.52
TRADES + LBGAT + TRAIN	<b>62.62</b> ( $\uparrow$ 2.19)	<b>36.27</b> ( $\uparrow$ 0.77)	<b>31.72</b> ( $\uparrow$ 0.22)	29.19( $\downarrow$ 0.15)	<b>64.84</b> ( $\uparrow$ 3.78)	<b>38.25</b> ( $\uparrow$ 0.73)

adversarial attack methods for evaluation: PGD-20, C&W-20 [53], and Auto Attack [54]. We denote the model’s defense success rate under those attacks separately as *PGD-20 Acc.*, *C&W-20 Acc.*, and *AA Acc.*. Similar to manifold learning, we make  $k$ NN test accuracy as a topology score due to  $k$ NN relying solely on the relationships among samples to classify. We utilize training sets as support sets (natural samples and adversarial samples generated by PGD-20) and methods [29], [47]. In Fig. 3 we set  $k$  as 5, 10, 20, 30, 40, 50, and we observe that the choice of  $k$  does not affect the relative ranking of the topological relationships among samples in different representation spaces. So in Tables I and II, we set  $k$  as 30.

**Data pre-process.** Similar to LBGAT [19], for CIFAR-10/100 datasets, the input size of each image is  $32 \times 32$ , and the training data is normalized to  $[0, 1]$  after standard data augmentation: random crops of 4 pixels padding size and random horizontal flip, and the test set is normalized to  $[0, 1]$  without any extra augmentation; For the training set of Tiny ImageNet, we resize the image from  $64 \times 64$  to  $32 \times 32$ , and the data augmentation is random crops with 4 pixels of padding; finally, we normalize pixel values to  $[0, 1]$ , and for the test set, we resize the image to  $32 \times 32$  and normalize pixel values to  $[0, 1]$ . Others are the same as CIFAR datasets.

**Training details.** For Table I, Table II, qualitative experiments, and all ablation experiments, we keep the same super-

parameter configuration as LBGAT. ResNet-18 is the backbone of standard models, and WideResNet-34-10 is the backbone of adversarial models. The adopted adversarial attacking method during training is PGD-10, with a perturbation size  $\epsilon = 0.031$ , a step size of perturbations  $\epsilon_1 = 0.007$ . The initial learning rate is set to 0.1 with a total of 100 epochs for training and reduced to 0.1x at the 75-th and 90-th epochs. The optimization algorithm is SGD, with a momentum of 0.9 and weight decay of  $2 \times 10^{-4}$ . For different experiment settings, we choose different  $\lambda$ . We set  $\lambda = 5$  on CIFAR-10 dataset, and  $\lambda = 20a$  on CIFAR-100 dataset, where  $a = \frac{2}{1 + e^{-\frac{10t}{100} - 1}}$  and  $t$  is the current  $t$ -th epoch during training. Moreover, all our experimental results are reproducible with a random seed of 1.

Furthermore, for Tables III and IV, we follow state-of-the-art adversarial training method LAS [26].  $\epsilon$  is 8/255. The initial learning rate is set to 0.1 with a total of 110 epochs for training and reduced to 0.1x at the 100-th and 105-th epochs. Weight decay is  $5 \times 10^{-4}$ . Others are the same as LBGAT. Finally, all experiments were done on GeForce RTX 3090, and we also provided our core code in the supplementary material, and all the existing assets we used chose an MIT license.

## B. Main Results

We conduct adequate quantitative analyses on CIFAR-10 and CIFAR-100. The results show that TRAIN can be combined

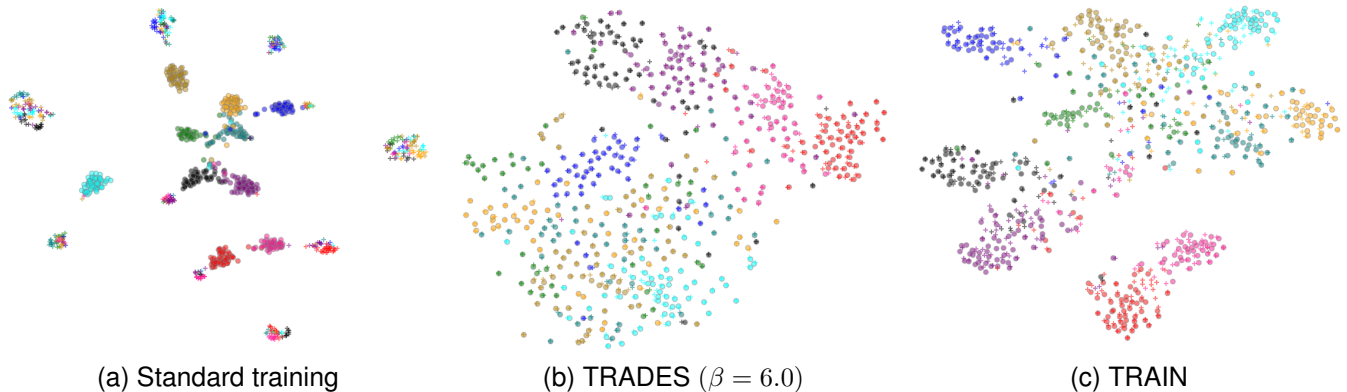


Fig. 5. t-SNE visualizations of penultimate layer features on CIFAR-10. A total of 512 samples are selected. Crosses and circles are adversarial samples and natural samples, respectively. Different colors represent different classes. TRAIN can enhance the topological preservation of natural samples while classifying adversarial samples correctly.

with other adversarial training algorithms in a plug-and-play way to improve the data topological structure of both natural and adversarial samples in the representation space. This improvement leads to an increase in both the accuracy of natural samples and the robustness against adversarial attacks. In addition, Tables I and II also demonstrate a strong positive correlation between the quality of topology and natural/robust accuracy. In the following, we will present the experimental results for each of the two datasets.

**Quantitative results.** According to Tables I and II, TRAIN can effectively increase both natural and robust accuracy, and contribute to the topology preservation of both natural and adversarial samples.

In Table I, TRAIN gets an improvement by 2.16% compared to vanilla AT baseline on natural data. It surpasses vanilla AT on PGD-20, C&W, and AA accuracy by 2.19%, 2.46%, and 1.94% respectively, indicating its high robustness. Our method also has improvements on LBGAT by 4.50% to 1.87% in all aspects. For another common baseline, TRADES, TRAIN also gets competitive results on both natural and adversarial data. Note that natural accuracy decreases when applying LBGAT to TRADES, so it also brings a large enhancement when combined with our method. For the topology score which is measured by  $k$ NN accuracy, TRAIN could boost the performance by a large margin. Since  $k$ NN classification is based only on inter-sample relationships, such results prove that TRAIN could mitigate topology disruptions of both natural and adversarial samples from adversarial training.

The overall results on CIFAR-100 are similar to CIFAR-10. As shown in Table II, TRAIN performs better than vanilla AT and LBGAT and gets a further improvement when deployed with LBGAT simultaneously. For TRADES, our method surpasses it by a large margin (8.78%) on natural data and improves the robust accuracy by 3.04%. Adding LBGAT to TRAIN causes a decrease in natural accuracy but achieves the best accuracy in PGD-20 and C&W-20. The above results show that the proposed TRAIN could be applied to popular adversarial training pipelines for achieving SOTA performance on both natural accuracy and robust accuracy. Despite a slight decrease in individual robust metrics, we have achieved a better

TABLE III  
RESULTS ON CIFAR-10. “\*” ARE THE RESULTS DIRECTLY QUOTED FROM LAS. THE BEST AND SECOND BEST RESULTS ARE **BOLDED** AND UNDERLINED, RESPECTIVELY.

Defense	Natural Acc.	PGD-20 Acc.	Robust Acc. C&W-20 Acc.	AA Acc.
Vanilla AT* [7]	85.17	55.08	53.91	51.69
MART* [32]	84.17	<u>58.56</u>	54.58	51.10
FAT* [25]	<b>87.97</b>	49.86	48.65	47.48
GAIRAT* [24]	86.30	<b>59.54</b>	45.57	40.30
AWP* [34]	85.57	58.13	56.03	53.90
TRADES* [10]	85.72	56.10	53.87	53.40
LAS-TRADES* [26]	85.24	57.07	55.45	54.15
TRADES + TRAIN	<u>87.07</u> ( $\uparrow$ 1.35)	<u>58.51</u> ( $\uparrow$ 2.41)	<b>56.81</b> ( $\uparrow$ 2.94)	<b>54.70</b> ( $\uparrow$ 1.30)
TRADES + LBGAT [19]	80.20	57.41	54.84	53.32
TRADES + LBGAT + TRAIN	86.69( $\uparrow$ 6.49)	58.04( $\uparrow$ 0.63)	<u>56.75</u> ( $\uparrow$ 1.91)	<u>54.47</u> ( $\uparrow$ 1.15)

balance between natural accuracy and adversarial robustness overall. For the topology score, we can find that combining the baseline with TRAIN can further enhance the quality of topology for both natural and adversarial samples in the representation space.

As shown in Tables III and IV, TRAIN achieves a better trade-off between natural accuracy and adversarial robustness compared with the most popular adversarial training algorithms. TRADES and LBGAT achieve significant improvement in natural accuracy by combining with TRAIN, and the robust accuracy is also relatively improved or preserved. Compared with the state-of-the-art method LAS-TRADES, we also have clear advantages on natural accuracy and adversarial robustness. Please note that the hyperparameter configuration in Table III and Table IV follows LAS, which differs from Table I and Table II. And our method exhibits superior performance when applied with the new hyperparameters.

**Qualitative analysis.** To showcase the efficacy of our algorithm in assisting the adversarial model in constructing a well-generalizing topology in the representation space, we use t-SNE to visualize samples from ten randomly selected categories in the CIFAR-100 test set and all categories of the CIFAR-10 test set for qualitative analysis. Figs. 2 and 5 show the results of CIFAR-100/10 datasets, respectively. For standard training (Figs. 2a and 5a), the natural data exhibit clear clustering, while the adversarial samples appear disjointed, resulting in



TABLE IV

RESULTS ON CIFAR-100. “\*” ARE THE RESULTS DIRECTLY QUOTED FROM LAS. THE BEST AND SECOND BEST RESULTS ARE MARKED IN **BOLD** AND UNDERLINE.

Defense	Natural Acc.	PGD-20 Acc.	Robust Acc. C&W-20 Acc.	AA Acc.
Vanilla AT* [7]	60.89	31.69	30.10	27.86
SAT* [52]	62.82	27.17	27.32	24.57
AWP* [34]	60.38	33.86	31.12	28.86
TRADES* [10]	58.61	28.66	27.05	25.94
LAS-TRADES* [26]	60.62	32.53	29.51	28.12
TRADES + TRAIN	<b>67.47</b> ( $\uparrow$ 8.86)	<u>34.99</u> ( $\uparrow$ 6.33)	<u>31.61</u> ( $\uparrow$ 4.56)	28.95( $\uparrow$ 3.01)
TRADES + LBGAT* [19]	60.64	34.75	30.65	29.33
TRADES + LBGAT+ TRAIN	<u>65.40</u> ( $\uparrow$ 4.76)	<b>35.46</b> ( $\uparrow$ 0.71)	<b>32.36</b> ( $\uparrow$ 1.71)	<b>30.17</b> ( $\uparrow$ 0.84)

TABLE V

QUANTITATIVE EXPERIMENT ON TINY IMAGENET. “\*” ARE THE RESULTS DIRECTLY QUOTED FROM LBGAT.

Defense	Clean Acc.	PGD-20 Acc.
Vanilla AT* [7]	30.65	6.81
Vanilla AT + LBGAT* [19]	36.50	14.00
ALP* [51]	30.51	8.01
LBGAT + ALP* [19]	33.67	14.55
TRADES ( $\beta = 6.0$ )* [10]	38.51	13.48
TRADES ( $\beta = 6.0$ ) + LBGAT* [19]	39.26	16.42
TRADES ( $\beta = 6.0$ ) + Ours	41.12( $\uparrow$ 2.61)	16.18( $\uparrow$ 2.70)
TRADES ( $\beta = 6.0$ ) + LBGAT+ Ours	<b>41.53</b> ( $\uparrow$ 2.27)	<b>17.09</b> ( $\uparrow$ 0.67)

poor performance on robust accuracy. The TRADES approach facilitates the alignment of natural and adversarial data to enhance robust accuracy. Nonetheless, it is noteworthy that this alignment process can unintentionally disrupt the integrity of natural feature topologies, as it lacks any defensive measures to counteract this effect (refer to Figs. 2b and 5b in the paper for visual representations of this phenomenon). As shown in Figs. 2c and 5c, applying the proposed TRAIN to TRADES could drive the cluster for each category to be more compact, thereby preserving the topology more effectively.

**Quantitative results on Tiny ImageNet.** To demonstrate the effectiveness of our approach on a highly demanding dataset, we performed rigorous experiments on the Tiny Imagenet dataset. The results, as depicted in Table V, clearly demonstrates that the combination of our algorithm with TRADES and LBGAT techniques leads to substantial improvements in both natural accuracy and adversarial robustness. When combined with Trades, our approach achieves a 2.61% improvement in natural accuracy and a 2.70% improvement in robust accuracy. When combined with TRADES+LBGAT, our method achieves a 2.27% improvement in natural accuracy and a 0.67% improvement in robust accuracy.

### C. Ablation Studies

In this section, we delve into TRAIN to study its effectiveness in different relation-preserving methods, batch size, hyper-parameter  $\lambda$ , and model architectures. We also analyze the time complexity and training time of our method. All the ablation experiments are based on the CIFAR-100 dataset and combined with TRADES. The experimental settings are the same as Tables I and II.

**Impact of relation-preserving methods.** In this section, we present a comparative analysis of our proposed method with alternative approaches: a metric learning approach called

TABLE VI

ABLATION RESULTS ON DIFFERENT RELATION-PRESERVING METHODS.

Methods	Natural Acc	Robust Acc		
		PGD-20 Acc	C&W-20 Acc	AA Acc
Vanilla AT [7]	60.44	28.06	27.85	24.81
MCA [55]	57.18	29.31	27.23	25.76
Vanilla AT + RKD [43]	64.00	28.32	27.92	24.92
Vanilla AT + CRD [56]	62.22	27.47	27.42	24.53
Vanilla AT + TRAIN	<b>66.39</b>	<b>29.88</b>	<b>29.84</b>	<b>25.81</b>

MCA [55] and two absolute relationship distillation methods, namely RKD [43] and CRD [56]. MCA applies a supervised contrastive loss into adversarial training. RKD takes the absolute value of the cosine distance between samples as the relationship as discussed in Sec. IV. To distill the structure of the teacher model in the representation space, CRD requires that a sample’s representation in the student model be closer to its corresponding representation in the teacher model while being farther from the representations of other samples in the teacher model.

**Impact of batch size.** As shown in Table VIII, we tried 128, 256, 384 samples per batch for relation calculating. Among them, a batch size of 256 achieves the best results, but the difference among different batch sizes is not large. Overall our method is not sensitive to different batch sizes.

To ensure fair comparisons with other methods, we chose a batch size of 128 for our other experiments.

**Sensitivity analysis of hyper-parameter  $\lambda$ .** As Table IX shows, with the increase of  $\lambda$  in Eq. 4, natural accuracy always gets higher;  $L_{TP}$  (calculated from the test set) gets lower; while the PGD-20 accuracy rises at first and then remains stable. It is reasonable because a large  $\lambda$  forces the topology of clean samples to be highly close to that of standard models. Finally, we set  $\lambda$  as  $20a$  according to the PGD-20 accuracy following [7].

**Time complexity.** Our method is based on batch computation, and its time complexity is  $O(N(mz'K)) + O(N(bz(fz' + fz) + mz))$ , where  $mz'$  and  $mz$  is the number of neurons of the adversarial model (48.32 M) and standard model (11.22 M),  $bz$  is the batch size (128),  $fz'$  and  $fz$  is the feature size of the standard model (512) and adversarial model (640), and  $K$  is the number of iterations for generating adversarial examples (10). For classic adversarial training, its time complexity is  $O(N(mz'K))$ . Since  $bz(fz' + fz) + mz \ll mz'K$ , the additional time overhead of our method is negligible.

Note that, the primary time-consuming factor in adversarial training algorithms lies in the need for additional backpropagation during the generation of adversarial samples, whereas the TRAIN algorithm does not incur any extra computational cost in this regard. Table XI shows the time statistics for training one epoch (with batch size equals 128) by different baselines. It takes additional 28 seconds when combined with Vanilla AT and 3% (30 seconds) on TRADES for TRAIN, which is as fast as LBGAT.

**Impact of the different standard models.** As depicted in Table VII, our approach exhibits robustness to variations in the backbones of standard models. Specifically, we observe that ResNet18 achieves a comparable trade-off between natural

TABLE VII  
THE ABLATION EXPERIMENT ABOUT DIFFERENT BACKBONES OF THE STANDARD MODEL.

Backbone of $M'$	Training Strategy	Backbone of $M$	Clean Acc.	Robust Acc.		
				PGD-20 Acc.	C&W-20 Acc.	AA Acc.
None	Standard Training	ResNet-18	77.39	0	0	0
WideResNet34-10	TRADES+Ours	ResNet-18	62.62	36.27	31.72	29.19
None	Standard Training	WideResNet34-10	78.11	0	0	0
WideResNet34-10	TRADES + Ours	WideResNet34-10	63.09	35.54	30.41	28.76

TABLE VIII  
THE ABLATION EXPERIMENT ABOUT DIFFERENT BATCH SIZES.

Batch Size	Natural Acc.	Robust Acc.		
		PGD-20 Acc.	C&W-20 Acc.	AA Acc.
128	66.39	29.88	29.84	25.81
256	<b>66.55</b>	<b>31.08</b>	<b>30.72</b>	<b>26.07</b>
384	66.26	30.60	30.16	25.41

TABLE IX  
SENSITIVITY ANALYSIS OF HYPER-PARAMETER  $\lambda$ .

	0	$5a$	$10a$	$20a$	$50a$
<b>Natural Acc.</b>	57.99	61.52	63.21	65.28	<b>66.40</b>
<b>PGD-20 Acc.</b>	31.53	32.31	33.47	<b>33.90</b>	33.62
$L_{TP}$	0.66	0.35	0.32	0.27	<b>0.24</b>

accuracy and adversarial robustness to WideresNet34-10 on the CIFAR-100 datasets while incurring lower training costs.

Table X shows the results of using different standard training strategies. To expedite the training process, a pre-trained standard model can be used in TRAIN (vanilla AT+TRAIN\*). However, training the standard model and adversarial model jointly achieves superior results. This is attributed to the fact that the representation spaces of the two joint models are closer, facilitating optimization procedures.

TABLE XII  
EXPERIMENTS USING MOBILENETV3 ON CIFAR100.

Methods	Clean Acc	Robust Acc		
		PGD-20 Acc	C&W-20 Acc	AA Acc
Vanilla AT	35.10	18.89	16.19	14.63
Vanilla AT+ TRAIN	38.58	20.25	17.64	15.39
TRADES	38.39	17.90	14.36	13.38
TRADES +TRAIN	43.64	18.52	14.86	13.51

**Impact of different backbones of  $M'$ .** We conduct experiments on MobileNetv3, and the results reinforce the effectiveness of our approach across different backbones. As shown in Table XII, our method can further improve the baseline, especially in natural accuracy. We achieve a maximum improvement of 5.25% in natural accuracy and a maximum improvement of 1.45% in robust accuracy.

We can also find that the experimental results on MobileNet v3 are inferior compared to WideResNet34-10, both in terms of robustness and natural sample accuracy. This observation can be attributed to the positive correlation between the effectiveness of adversarial training algorithms and model capacity [57], and

TABLE X  
ABLATION EXPERIMENT ABOUT DIFFERENT STANDARD MODELS ON CIFAR-100. TRAIN\* MEANS USING A WELL-TRAINED STANDARD MODEL, AND TRAIN MEANS TRAINING TWO MODELS JOINTLY.

Methods	Clean Acc	Robust Acc		
		PGD-20 Acc	C&W-20 Acc	AA Acc
Vanilla AT	60.44	28.06	27.85	24.81
Vanilla AT + TRAIN*	65.15	28.00	27.90	24.91
Vanilla AT + TRAIN	<b>66.39</b>	<b>29.88</b>	<b>29.84</b>	<b>25.81</b>

TABLE XI  
TRAINING TIME IN SECOND OF AN EPOCH ON ONE RTX 3090 GPU.

Vanilla AT	Vanilla AT + LBGAT	Vanilla AT + TRAIN
821	848	849
TRADES	TRADES + LBGAT	TRADES + TRAIN
1,079	1,106	1,109

to reduce inference speed, MobileNet v3 has a significantly smaller model capacity compared to WideResNet34-10.

## VI. CONCLUSIONS AND FUTURE WORK

Compared with standard training, adversarial training shows significant natural accuracy degradation. Different from previous algorithms, we assume this is due to topology disruption of natural features, and confirm it by empirical experiments. Based on that, we propose Topology-pReserving Adversarial traINing (TRAIN). While improving the adversarial robustness of the model, it preserves the topology of natural samples in the representation space of the standard model. Because the adversarial training will make the natural samples close to the feature distribution of their generated adversarial samples, TRAIN can also improve the quality of the topology of adversarial samples. On the CIFAR-10 and CIFAR-100 datasets, we get a maximum improvement of 8.78% in natural sample accuracy and 4.50% in robust accuracy, and visualizations justify that TRAIN does help the adversarial model to constitute a better topological structure of samples.

There are a few future directions we plan to explore. TRAIN is only related to the representation space regardless of the label space and the model backbone, so it can be combined with unsupervised learning methods in nature, and using different standard models as guided even across modalities.

## REFERENCES

- [1] F. Zhang, P. P. K. Chan, B. Biggio, D. S. Yeung, and F. Roli, "Adversarial feature selection against evasion attacks," *IEEE Transactions on Cybernetics*, vol. 46, no. 3, pp. 766–777, 2016.
- [2] E. Yang, T. Liu, C. Deng, and D. Tao, "Adversarial examples for hamming space search," *IEEE Transactions on Cybernetics*, vol. 50, no. 4, pp. 1473–1484, 2020.
- [3] H. Shen, S. Chen, R. Wang, and X. Wang, "Adversarial learning with cost-sensitive classes," *IEEE Transactions on Cybernetics*, pp. 1–12, 2022.
- [4] Z. Wang, X. Shu, Y. Wang, Y. Feng, L. Zhang, and Z. Yi, "A feature space-restricted attention attack on medical deep learning systems," *IEEE Transactions on Cybernetics*, pp. 1–13, 2022.
- [5] D. Wang, C. Li, S. Wen, Q.-L. Han, S. Nepal, X. Zhang, and Y. Xiang, "Daedalus: Breaking nonmaximum suppression in object detection via adversarial examples," *IEEE Transactions on Cybernetics*, vol. 52, no. 8, pp. 7427–7440, 2022.
- [6] C. Szegedy, W. Zaremba, I. Sutskever, J. Bruna, D. Erhan, I. Goodfellow, and R. Fergus, "Intriguing properties of neural networks," in *International Conference on Learning Representations (ICLR)*, 2014.
- [7] A. Madry, A. Makelov, L. Schmidt, D. Tsipras, and A. Vladu, "Towards deep learning models resistant to adversarial attacks," *arXiv preprint arXiv:1706.06083*, 2017.
- [8] C. Xie, J. Wang, Z. Zhang, Z. Ren, and A. Yuille, "Mitigating adversarial effects through randomization," *arXiv preprint arXiv:1711.01991*, 2017.
- [9] G. S. Dhillon, K. Azizzadenesheli, Z. C. Lipton, J. Bernstein, J. Kossaiifi, A. Khanna, and A. Anandkumar, "Stochastic activation pruning for robust adversarial defense," *arXiv preprint arXiv:1803.01442*, 2018.
- [10] H. Zhang, Y. Yu, J. Jiao, E. Xing, L. El Ghaoui, and M. Jordan, "Theoretically principled trade-off between robustness and accuracy," in *International conference on machine learning*. PMLR, 2019, pp. 7472–7482.
- [11] P. Bashivan, R. Bayat, A. Ibrahim, K. Ahuja, M. Faramarzi, T. Laleh, B. Richards, and I. Rish, "Adversarial feature desensitization," *Advances in Neural Information Processing Systems*, vol. 34, 2021.
- [12] A. Sarkar, A. Sarkar, S. Gali, and V. N. Balasubramanian, "Get fooled for the right reason: Improving adversarial robustness through a teacher-guided curriculum learning approach," *arXiv preprint arXiv:2111.00295*, 2021.
- [13] L. Schott, J. Rauber, M. Bethge, and W. Brendel, "Towards the first adversarially robust neural network model on mnist," *arXiv preprint arXiv:1805.09190*, 2018.
- [14] P. Maini, E. Wong, and Z. Kolter, "Adversarial robustness against the union of multiple perturbation models," in *International Conference on Machine Learning*. PMLR, 2020, pp. 6640–6650.
- [15] T. Pang, X. Yang, Y. Dong, H. Su, and J. Zhu, "Bag of tricks for adversarial training," in *International Conference on Learning Representations*, 2021.
- [16] T. Pang, M. Lin, X. Yang, J. Zhu, and S. Yan, "Robustness and accuracy could be reconcilable by (proper) definition," 2022.
- [17] A. Athalye, N. Carlini, and D. Wagner, "Obfuscated gradients give a false sense of security: Circumventing defenses to adversarial examples," in *International conference on machine learning*. PMLR, 2018, pp. 274–283.
- [18] F. Tramer, N. Carlini, W. Brendel, and A. Madry, "On adaptive attacks to adversarial example defenses," *Advances in Neural Information Processing Systems*, vol. 33, pp. 1633–1645, 2020.
- [19] J. Cui, S. Liu, L. Wang, and J. Jia, "Learnable boundary guided adversarial training," in *Proceedings of the IEEE/CVF International Conference on Computer Vision*, 2021, pp. 15721–15730.
- [20] P. Huang, Y. Yang, M. Liu, F. Jia, F. Ma, and J. Zhang, " $\epsilon$ -weakened robustness of deep neural networks," in *Proceedings of the 31st ACM SIGSOFT International Symposium on Software Testing and Analysis*, ser. ISSTA 2022. New York, NY, USA: Association for Computing Machinery, 2022, p. 126–138. [Online]. Available: <https://doi.org/10.1145/3533767.3534373>
- [21] S.-A. Rebuffi, S. Gowal, D. A. Calian, F. Stimberg, O. Wiles, and T. A. Mann, "Data augmentation can improve robustness," *Advances in Neural Information Processing Systems*, vol. 34, pp. 29935–29948, 2021.
- [22] E. Arani, F. Sarfraz, and B. Zonooz, "Adversarial concurrent training: Optimizing robustness and accuracy trade-off of deep neural networks," *arXiv preprint arXiv:2008.07015*, 2020.
- [23] E.-C. Chen and C.-R. Lee, "Ltd: Low temperature distillation for robust adversarial training," *arXiv preprint arXiv:2111.02331*, 2021.
- [24] J. Zhang, J. Zhu, G. Niu, B. Han, M. Sugiyama, and M. S. Kankanhalli, "Geometry-aware instance-reweighted adversarial training," in *ICLR*, 2021.
- [25] J. Zhang, X. Xu, B. Han, G. Niu, L. Cui, M. Sugiyama, and M. Kankanhalli, "Attacks which do not kill training make adversarial learning stronger," in *International conference on machine learning*. PMLR, 2020, pp. 11278–11287.
- [26] X. Jia, Y. Zhang, B. Wu, K. Ma, J. Wang, and X. Cao, "Las-at: Adversarial training with learnable attack strategy," in *Proceedings of the IEEE/CVF Conference on Computer Vision and Pattern Recognition*, 2022, pp. 13398–13408.
- [27] J. R. Rabunal, J. Dorado, and A. P. Sierra, *Encyclopedia of artificial intelligence*. IGI Global, 2009.
- [28] M. Belkin, P. Niyogi, and V. Sindhwani, "Manifold regularization: A geometric framework for learning from labeled and unlabeled examples," *Journal of machine learning research*, vol. 7, no. 11, 2006.
- [29] L. McInnes, J. Healy, and J. Melville, "UMAP: Uniform Manifold Approximation and Projection for Dimension Reduction," *arXiv preprint arXiv:1802.03426*, 2018.
- [30] C. Zhang, N. Song, G. Lin, Y. Zheng, P. Pan, and Y. Xu, "Few-shot incremental learning with continually evolved classifiers," in *Proceedings of the IEEE/CVF Conference on Computer Vision and Pattern Recognition*, 2021, pp. 12455–12464.
- [31] C. Mao, Z. Zhong, J. Yang, C. Vondrick, and B. Ray, "Metric learning for adversarial robustness," *Advances in Neural Information Processing Systems*, vol. 32, 2019.
- [32] Y. Wang, D. Zou, J. Yi, J. Bailey, X. Ma, and Q. Gu, "Improving adversarial robustness requires revisiting misclassified examples," in *International Conference on Learning Representations*, 2019.
- [33] E. Wong, L. Rice, and J. Z. Kolter, "Fast is better than free: Revisiting adversarial training," *arXiv preprint arXiv:2001.03994*, 2020.
- [34] D. Wu, S.-T. Xia, and Y. Wang, "Adversarial weight perturbation helps robust generalization," *Advances in Neural Information Processing Systems*, vol. 33, pp. 2958–2969, 2020.
- [35] T. Li, Y. Wu, S. Chen, K. Fang, and X. Huang, "Subspace adversarial training," *arXiv preprint arXiv:2111.12229*, 2021.
- [36] G. Hinton, O. Vinyals, J. Dean *et al.*, "Distilling the knowledge in a neural network," *Advances in Neural Information Processing Systems Workshop*, vol. 2, no. 7, 2014.
- [37] I. Sucholutsky and M. Schonlau, "Soft-label dataset distillation and text dataset distillation," in *2021 International Joint Conference on Neural Networks (IJCNN)*. IEEE, 2021, pp. 1–8.
- [38] A. Romero, N. Ballas, S. E. Kahou, A. Chassang, C. Gatta, and Y. Bengio, "Fitnets: Hints for thin deep nets," *arXiv preprint arXiv:1412.6550*, 2014.
- [39] I.-J. Liu, J. Peng, and A. G. Schwing, "Knowledge flow: Improve upon your teachers," *arXiv preprint arXiv:1904.05878*, 2019.
- [40] P. Chen, S. Liu, H. Zhao, and J. Jia, "Distilling knowledge via knowledge review," in *Proceedings of the IEEE/CVF Conference on Computer Vision and Pattern Recognition*, 2021, pp. 5008–5017.
- [41] N. Passalis and A. Tefas, "Learning deep representations with probabilistic knowledge transfer," in *Proceedings of the European Conference on Computer Vision (ECCV)*, 2018, pp. 268–284.
- [42] F. Tung and G. Mori, "Similarity-preserving knowledge distillation," in *Proceedings of the IEEE/CVF International Conference on Computer Vision*, 2019, pp. 1365–1374.
- [43] W. Park, D. Kim, Y. Lu, and M. Cho, "Relational knowledge distillation," in *Proceedings of the IEEE/CVF Conference on Computer Vision and Pattern Recognition*, 2019, pp. 3967–3976.
- [44] J. Zhu, S. Tang, D. Chen, S. Yu, Y. Liu, M. Rong, A. Yang, and X. Wang, "Complementary relation contrastive distillation," in *Proceedings of the IEEE/CVF Conference on Computer Vision and Pattern Recognition*, 2021, pp. 9260–9269.
- [45] M. Goldblum, L. Fowl, S. Feizi, and T. Goldstein, "Adversarially robust distillation," in *Proceedings of the AAAI Conference on Artificial Intelligence*, vol. 34, no. 04, 2020, pp. 3996–4003.
- [46] B. Zi, S. Zhao, X. Ma, and Y.-G. Jiang, "Revisiting adversarial robustness distillation: Robust soft labels make student better," in *Proceedings of the IEEE/CVF International Conference on Computer Vision*, 2021, pp. 16443–16452.
- [47] L. Van der Maaten and G. Hinton, "Visualizing data using t-SNE," *Journal of machine learning research*, vol. 9, no. 11, 2008.
- [48] X. Tao, X. Chang, X. Hong, X. Wei, and Y. Gong, "Topology-preserving class-incremental learning," in *European Conference on Computer Vision*. Springer, 2020, pp. 254–270.
- [49] A. Krizhevsky, G. Hinton *et al.*, "Learning multiple layers of features from tiny images," 2009.

- [50] J. Deng, W. Dong, R. Socher, L.-J. Li, K. Li, and L. Fei-Fei, “Imagenet: A large-scale hierarchical image database,” in *2009 IEEE conference on computer vision and pattern recognition*. Ieee, 2009, pp. 248–255.
- [51] H. Kannan, A. Kurakin, and I. Goodfellow, “Adversarial logit pairing,” *arXiv preprint arXiv:1803.06373*, 2018.
- [52] C. Sitawarin, S. Chakraborty, and D. Wagner, “Sat: Improving adversarial training via curriculum-based loss smoothing,” in *Proceedings of the 14th ACM Workshop on Artificial Intelligence and Security*, 2021, pp. 25–36.
- [53] N. Carlini and D. Wagner, “Towards evaluating the robustness of neural networks,” in *2017 IEEE Symposium on Security and Privacy (SP)*. IEEE, 2017, pp. 39–57.
- [54] F. Croce and M. Hein, “Reliable evaluation of adversarial robustness with an ensemble of diverse parameter-free attacks,” in *International conference on machine learning*. PMLR, 2020, pp. 2206–2216.
- [55] S. Yang, Z. Feng, P. Du, B. Du, and C. Xu, “Structure-aware stabilization of adversarial robustness with massive contrastive adversaries,” in *2021 IEEE International Conference on Data Mining (ICDM)*. IEEE, 2021, pp. 807–816.
- [56] Y. Tian, D. Krishnan, and P. Isola, “Contrastive representation distillation,” in *International Conference on Learning Representations*, 2019.
- [57] T. Bai, J. Luo, J. Zhao, B. Wen, and Q. Wang, “Recent advances in adversarial training for adversarial robustness,” *arXiv preprint arXiv:2102.01356*, 2021.